ELSEVIER

Biochimica et Biophysica Acta 1559 (2002) 145–159

BIOCHIMICA ET BIOPHYSICA ACTA

BBA

www.bba-direct.com

Modes of membrane interaction of a natural cysteine-rich peptide: viscotoxin A3

Alexandre Coulon [a], Emir Berkane [a], Anne-Marie Sautereau [a], Konrad Urech [b], Pierre Rougé [a], André Lopez [a,*]

[a] *Institut de Pharmacologie et de Biologie Structurale, UMR-CNRS 5089, 205 Route de Narbonne, 31077 Toulouse Cedex 4, France*

[b] *Verein für Krebsforschung, Hiscia Institut, CH 4144 Arlesheim, Switzerland*

Received 9 October 2001; received in revised form 15 November 2001; accepted 22 November 2001

Abstract

Among the very homologous family of α- and β-thionins, known for their antimicrobial activity, the viscotoxin subfamily differs from other members because it is cytotoxic against tumoral cells but weakly hemolytic. We studied the interactions between the most active of these toxins, viscotoxin A3 (VA3), and model membranes made of phosphatidylcholine and phosphatidylserine (PS), the major zwitterionic and acidic phospholipids found in eukaryotic cells. Monolayer studies showed that electrostatic forces are essential for the interaction and are mainly involved in modulating the embedding of the toxin in the PS head group region. This in turn induces membrane stiffening, as shown by fluorescence polarization assays with 1,6-diphenyl-1,3,5-hexatriene and its derivatives. Moreover, vesicle permeabilization analyses showed that there are two modes of interaction, which are directly related to the stiffening effect and depend on the amount of VA3 bound to the surface of the vesicles. We propose an interaction model in which the embedding of VA3 in the membrane induces membrane defects leading to the gradual release of encapsulated dye. When the surfaces of the vesicles are saturated with the viscotoxin, complete vesicle destabilization is induced which leads to bilayer disruption, all-or-none encapsulated dye release and rearrangement of the vesicles.

Keywords: Viscotoxin; Thionin; Membrane; Phosphatidylserine; Release; Polarization

1. Introduction

Previous studies on natural membrane-active peptides have been mainly performed to find substitutes to overcome the increasing resistance of pathogenic bacteria towards antibiotics or antifungal drugs. However, some of these peptides are toxic to eukaryotic cells, especially tumoral cells, which means that they may be of great use for the development of cancer therapy. It has been shown that the five very homologous types of α- and β-thionin have very different activities, even though their overall three-dimensional structure appears to be highly con-

Abbreviations: CF, 5-(and 6)-carboxyfluorescein; CMC, critical micellar concentration; DPH, 1,6-diphenyl-1,3,5-hexatriene; β-DPH-HPC, 2-(3-(diphenylhexatrienyl)propanoyl)-1-hexadodecanoyl-*sn*-glycero-3-phosphocholine; EDTA, ethylenediaminetetraacetic acid; $LUVET_{100}$, large unilamellar vesicle of 100 nm diameter obtained by extrusion; MLV, multilamellar vesicle; MOPS, 3-(*N*-morpholino)propanesulfonic acid; NMR, nuclear magnetic resonance; NPN, *N*-phenyl-1-naphthylamine; POPC, 1-palmitoyl-2-oleoyl-*sn*-glycero-3-phosphocholine; POPS, 1-palmitoyl-2-oleoyl-*sn*-glycero-3-phospho-L-serine; QELS, quasi-elastic light scattering; TX100, Triton X-100; VA3, viscotoxin A3

* Corresponding author. Fax: +33-61-17-59-94.

E-mail address: andre.lopez@ipbs.fr (A. Lopez).

0005-2736/02/$ – see front matter
PII: S0005-2736(01)00446-1

served [1–4]. Type I and II thionins exhibit toxic effects on Gram-positive and Gram-negative bacteria and fungi, whereas type III and IV thionins do not inhibit growth in vitro [5–8]. Interestingly, type I and II thionins are highly toxic to many mammalian cell lines [5,7,9]. Viscotoxins, the thionins from mistletoe (*Viscum album*), belong to type III and display similar toxic activities towards a number of tumor cell lines [10–12]. The latter membrane-active peptides are potential anti-cancer drugs.

Although few studies have compared the in vitro activity of viscotoxins with that of other thionins, viscotoxins are known to be more toxic to eukaryotic cells than other thionins. ED_{50} values measured on human tumor HeLa cells were in the range of 0.2–1.7 μg ml^{-1} for viscotoxins [10] and 17 μg ml^{-1} for the *Pyrularia* thionin [13], respectively. Similarly, the incubation of human cultured lymphocytes with 50 μg ml^{-1} viscotoxins for 24 h caused some cell death, whereas no lethal effect was reported for purothionin [14]. Conversely, viscotoxins are far less hemolytic than other thionins. Under the same experimental conditions, 20 μg ml^{-1} *Pyrularia* thionin lysed 50% of human erythrocytes [15,16], whereas 100 μg ml^{-1} viscotoxin B only caused 10% hemolysis [17]. Viscotoxin A3 (VA3) (100 μg ml^{-1}) provoked a weak hemolysis (≤10%) of rabbit erythrocytes (unpublished data) whereas Osario e Castro et al. [18] reported that less than 10 μg ml^{-1} *Pyrularia* thionin lysed 21%.

Despite these striking differences, little attention has been paid to the mechanism of action of viscotoxins. Studies on thionins suggest that most of their toxic effects probably result from their direct interaction with the cell plasma membrane. Although attempts to isolate specific protein receptors for thionins from different types of target cells have failed [15], major changes in the structure of the plasma membrane have been reported to occur upon interaction with thionins [7,9,15,19]. Moreover, there is a correlation between the toxicity of thionins and their ability to induce the permeabilization of the target cells [8]. Results from model membranes strengthened this finding [6–8,20–22]. However, the molecular mechanism behind the toxicity of thionins remains controversial. According to Hughes et al. [7], thionins create ion channels within the plasma membrane. However, other studies suggest a peptide-induced destabilization of the membrane [8,20].

We studied the interactions between viscotoxin A3 and model membranes. VA3 (KSCCPNTTG^{10}R-NIYNACRLT^{20}GAPRPTCAKL^{30}SGCKIISGST^{40}-CPSDYPK), a cationic 46-amino acid peptide isolated from the leaves and stems of European mistletoe (*V. album*, Loranthaceae), is believed to be the most active of the viscotoxin isoforms [23]. We used monolayers built from different phospholipid types to show that VA3 has a high affinity for acidic phospholipids and to characterize the interaction as a partial insertion process. Experiments on vesicles made of 1-palmitoyl-2-oleoyl-*sn*-glycero-3-phospho-L-serine (POPS), the major acidic phospholipid of the eukaryotic plasma membrane, showed that VA3 promotes distinct permeabilizing effects on POPS vesicles depending on the VA3/POPS ratio. Furthermore, fluorescence polarization measurements provided some insight into the effects of VA3 on the overall organization of the lipid bilayer. Finally, the biological relevance of a proposed interaction model is discussed.

2. Materials and methods

2.1. Chemicals

POPS and 1-palmitoyl-2-oleoyl-*sn*-glycero-3-phosphocholine (POPC) were purchased from Avanti Polar Lipids (Alabaster, AL, USA). 5-(and 6)-Carboxyfluorescein (CF), 1,6-diphenyl-1,3,5-hexatriene (DPH) and 2-(3-(diphenylhexatrienyl)propanoyl)-1-hexadodecanoyl-*sn*-glycero-3-phosphocholine (β-DPH-HPC) were from Molecular Probes (Eugene, OR, USA). 3-(*N*-Morpholino)propanesulfonic acid (MOPS), sodium azide (NaN_3) and Triton X-100 (TX100) were obtained from Fluka (Buchs, Switzerland). *N*-Phenyl-1-naphthylamine (NPN) was purchased from Eastman Kodak (Rochester, NY, USA). Ethylenediaminetetraacetic acid (EDTA) was from Sigma-Aldrich (St.-Quentin, France). Other chemicals were of analytical grade. VA3 was isolated and purified from European mistletoe leaves as previously described [23].

VA3 stock solutions and all other aqueous solutions were gravimetrically prepared with MilliQ (Millipore) ultrapure water. POPC and POPS were stored as stock solutions in chloroformic solution

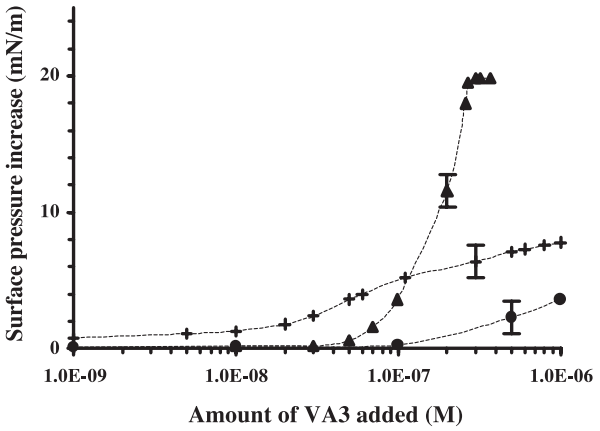

Fig. 1. Increase in surface pressure upon adding VA3 to the subphase with (▲,+) or without (●) a phospholipidic film at the interface. The films were made of POPS (▲) or POPC (+) and the initial pressure was 10 mN m^{-1}.

($CHCl_3$/MeOH, 9:1, v/v) and POPS was used within 24 h. Lipid purity was routinely controlled by thin layer chromatography on silica gel plates with $CHCl_3$/MeOH/H_2O (65:25:4, v/v/v) as the eluent. Phospholipid concentrations were estimated by phosphate assay subsequent to total digestion in the presence of perchloric acid [24].

2.2. Monolayer experiments

Isochoric measurements were performed in a circular Teflon trough with a 16 cm^2 area containing 10 ml subphase (10 mM MOPS, 100 mM NaCl, pH 7.4), by use of a Wilhelmy platinum plate connected to a home-made electrical torsion balance to measure the surface pressure. The atmosphere was saturated with water to prevent evaporation of the subphase during the experiment and the temperature was maintained at 21 ± 2°C. Films with an initial surface pressure of 10 mN m^{-1} were obtained by successively depositing the assayed chloroformic lipid solution. After a lag time of 30 min to allow the evaporation of the solvent and equilibration of the surface pressure, 10 or 20 μl of the VA3 aqueous solutions were introduced below the lipidic monolayer through a side hole, using a syringe (1 μl; Hamilton, Bonaduz, Switzerland). After 2 min of gentle stirring, another lag time of 15 min was observed to allow equilibration. For every 100 μl of VA3 solution injected, an equal subphase volume was carefully drawn off to avoid systematic error measurements of the surface pressure.

Compression isotherms were obtained as previously described [25], by use of a laboratory-made apparatus and a Wilhelmy platinum plate to determine the surface pressure. Briefly, about 10 nmoles of chloroformic lipid solution were carefully deposited on the aqueous phase (10 mM MOPS, 1, 150 or 300 mM NaCl, pH 7.4), to the left of the Teflon barrier and a 30 min lag time was observed to allow the solvent to evaporate. One hundred microliters of a 0.1 mM VA3 solution were then injected under the lipid monolayer to the right of the Teflon barrier. After 2 min of gentle stirring and a 30 min lag period, compression was performed from right to left at 4 $Å^2$ min^{-1}.

2.3. Preparation of large unilamellar vesicles by extrusion ($LUVET_{100}$)

Lipids were solubilized in chloroformic solutions and the organic solvents were thoroughly removed first by evaporation under nitrogen and then, overnight, under vacuum (1 Torr). The dry lipid mixture was dispersed in the standard buffer solution (10 mM MOPS, 150 mM NaCl, 1 mM EDTA, 0.02% NaN_3 (w/v), pH 7.4) to a final lipid concentration of 1 mg ml^{-1}. After a 30 min lag period to ensure proper lipid hydration, the mixture was strongly vortexed for 4 min to obtain multilamellar vesicles (MLV). $LUVET_{100}$ were prepared according to the extrusion method of Hope et al. [26] by use of a mini-extruder (Avanti Polar Lipids). Briefly, MLV dispersions were passed 45 times through two stacked polycarbonate

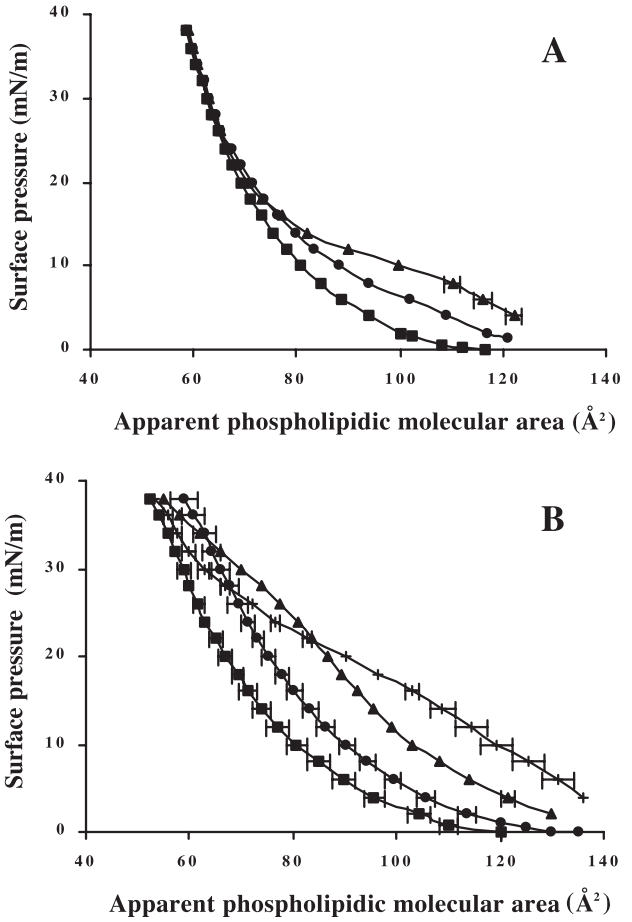

Fig. 2. Compression isotherms of POPC (A) and POPS (B) monomolecular films. These isotherms were recorded without (■) or with VA3 (0.1 μM) in the subphase, in buffers with different ionic strength modulated by the concentration of NaCl: 1 (●), 150 (▲) or 300 mM (+). Each curve is the result of at least three experiments.

filters with a pore size of 0.1 μm. Two drain disks were placed on both sides of each polycarbonate membrane. As the fluid to gel phase transition of POPS occurs at 6–13°C, both the extrusion procedure and the subsequent vesicle conservation were performed at room temperature to maintain POPS in the fluid phase. The size distribution of the vesicles was checked by quasi-elastic light scattering (QELS) on a 2C autosizer (Malvern, UK). Between 33 and 45 extrusion cycles, $LUVET_{100}$ exhibited a monomodal size distribution with a mean diameter of 106 ± 16 nm.

For fluorescence polarization measurements, DPH or β-DPH-HPC probes were added to a concentration of 1% to the chloroformic lipid solution prior to evaporation under nitrogen. A buffer containing additional 33.3 mM CF was used for the CF release assays. Non-encapsulated fluorescent probes were separated from the vesicles by filtering the vesicles through a column (19 cm × 1.3 cm) of Sephadex G-50 (Pharmacia) using the standard buffer as the eluent. This allowed us to obtain stable POPS vesicles showing less than 8% CF release over a period of 5 days. In selected experiments, freeze–thaw cycles were repeated five times before the extrusion procedure described and results were indistinguishable from those obtained without freeze–thaw cycles.

2.4. Fluorescence polarization

Fluorescence polarization was measured on a laboratory-made automatic T-format apparatus, as described previously [27]. $LUVET_{100}$ labeled with DPH or β-DPH-HPC were diluted in standard buffer to obtain a lipid concentration of 25 or 50 μM, that gave an absorbance value of less than 0.08 at 428 or 452 nm. Different amounts of VA3 were added to the $LUVET_{100}$ suspension and after incubation at 21 ± 2°C for 10 min with constant stirring, samples were put in a thermostat controlled housing device (Peltier unit) so that the temperature of the samples could be monitored. The temperature was then raised stepwise from 4 to 22°C at a rate of 0.5°C per 3 min. Fluorescence anisotropy is given by $r = (I_V + I_H)/(I_V + 2I_H)$, where I is the fluorescence intensity, and the subscripts indicate the vertical (V) or horizontal (H) orientation of the emission polarizer.

2.5. Binding assays

Various amounts of VA3 and $LUVET_{100}$ in standard buffer, corresponding to different protein/lipid molar ratios, were incubated in polycarbonate tubes (Beckman) with continuous stirring, at 21 ± 2°C for 20 min. The total volume was 2 ml. Bound and free proteins were separated by centrifugation (100 000 rpm, 20°C, 2 h) in a Beckman Optima TLX ultracentrifuge, using a TLA-100 rotor. Control experiments showed that less than 5% of the lipids remained in the upper 1.5 ml of the supernatant. Under the same experimental conditions, VA3 alone did not appreciably sediment at the bottom of the tubes but was significantly adsorbed onto the tube

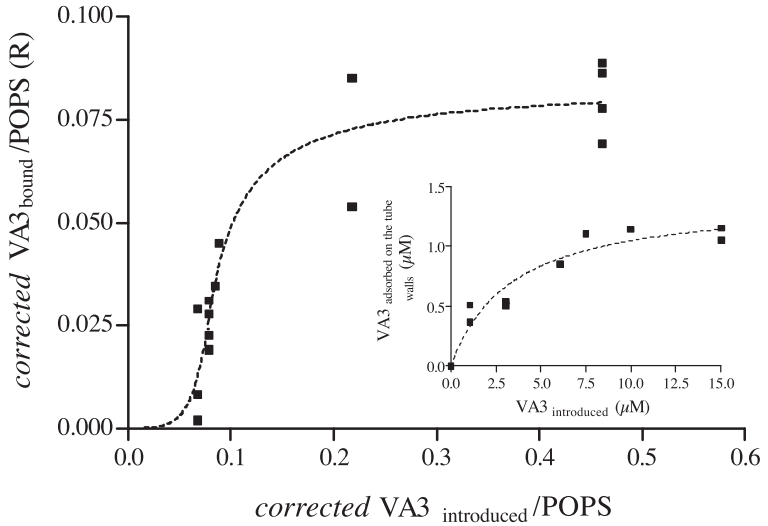

Fig. 3. Binding of VA3 on pure POPS $LUVET_{100}$. The *X*-axis values were calculated from the wall adsorption curve (insert). Due to strong wall adsorption no accurate data could be recorded for low VA3 concentrations. The lipid concentrations were 10, 30, 60, and 100 μM. The toxin apparent concentrations were between 1 and 15 μM. An apparent binding affinity < 3 μM has been estimated.

wall. We thus had to be able to determine the amount of free toxin, the amount bound to the $LUVET_{100}$ and the amount adsorbed on the tube wall.

To estimate the amount of toxin adsorbed to the wall, we incubated various amounts of VA3 in polycarbonate tubes, but in the absence of $LUVET_{100}$ and without centrifugation. VA3 samples were evaporated under nitrogen to eliminate the buffer and their protein content was estimated with the bicinchoninic acid assay (micro-BCA kit, Pierce, Rockford, IL, USA), by measuring the absorbance at 560 nm (A_{560}) on a Perkin-Elmer UV/VIS Lambda 16 spectrometer. In parallel, identical starting amounts of VA3 were diluted in standard buffer and titrated by the same approach. The ratio of the two corresponding A_{560} measurements was used to calculate the fraction of toxin not adsorbed on the tube wall.

The amount of toxin bound to $LUVET_{100}$ was estimated as follows. Various amounts of VA3 and $LUVET_{100}$ were incubated in parallel with control tubes containing identical amounts of VA3. After centrifugation, samples from the assay and control tubes were concentrated and their protein content was estimated colorimetrically at 560 nm. The ratio of the two corresponding A_{560} measurements was used to calculate the *apparent* unbound VA3 fraction. We used the amount of VA3 adsorbed to the wall to calculate the *corrected* VA3 fraction bound to $LUVET_{100}$.

2.6. CF release assay

Experiments were performed on $LUVET_{100}$ with encapsulated CF. The CF release assay is based on the fluorescence quenching this probe displays at high concentration [28]. CF release was estimated fluorometrically by monitoring the decrease in the self-quenching activity of the probe on an Aminco SPF 500C spectrofluorometer, with excitation and emission wavelengths set at 493 and 517 nm, respectively, and a band-pass slit of 2.5 nm.

Kinetic experiments were usually initiated by injecting 5–30 μl of VA3 stock solutions (0.1 or 1 mM) in a set of 2 ml quartz cuvettes containing known amounts of lipids (10, 30, 60 and 100 μM). At a constant temperature of 21 ± 1°C, the cuvettes were continuously stirred and shielded from light source to avoid CF photobleaching. The fluorescence of each cuvette was periodically monitored over a 50 s period. The maximum fluorescence was measured by adding 20 μl of a 10% (v/v) TX100 solution to each cuvette. Progress in the release is expressed as the percentage of CF release (%*F*) calculated from $[(I_t - I_0)/(I_{max} - I_0)]$ 100, where I_t is fluorescence intensity at time t, I_0 is background fluorescence of the

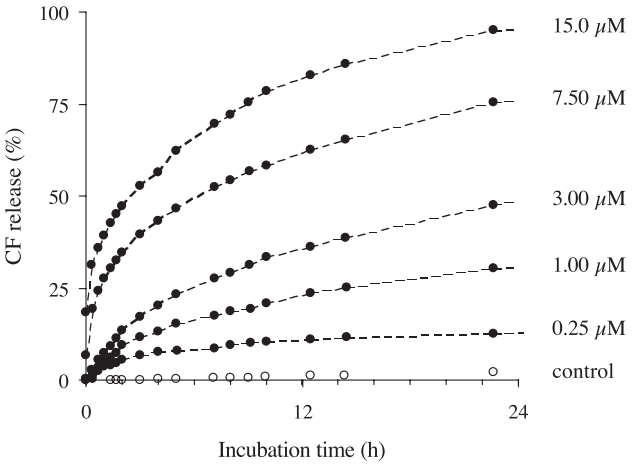

Fig. 4. POPS $LUVET_{100}$ permeabilization induced by varying the apparent concentrations of VA3. The total lipid concentration was 30 μM.

vesicles, and I_{max} is fluorescence measured after the addition of TX100.

We selected concentrations of lipids and encapsulated CF to ensure the complete release of the dye in infinitely diluted conditions, in order to obtain a linear relation between the fluorescence intensity and the free CF concentration. In addition, both the stability of $LUVET_{100}$ and the possible photobleaching of the probe were systematically investigated in all experiments. Under our experimental conditions, negligible photobleaching of the probe was measured.

2.7. Mode of dye release

To investigate the mode of the VA3-induced CF release from $LUVET_{100}$, the theoretical approach described by Weinstein et al. [28] was used. Briefly, different amounts of VA3 were added to 30 μM of CF-loaded $LUVET_{100}$ and the CF release was monitored as previously described. After a CF release $\approx 50\%$ was achieved, a 1 ml sample of the mixture was quickly filtered through the Sephadex G-50 column as described above, to eliminate the released dye. We performed a fluorometric analysis of the vesicle fraction with and without TX100 to estimate the percentage of fluorescence quenching ($\%Q_r$) remaining in the vesicles, according to: $\%Q_r = (1-I_0/I_{max})$. The residual intravesicular concentration of CF ($[CF]_r$) was calculated from the standard quench curve obtained by measuring the fluorescence quenching of vesicle samples prepared in standard buffer solutions containing 8.3–33.3 mM CF. This enabled us to calculate the equivalent gradual release ($\%F_{gr}$) that would have led to the same results, according to: $\%F_{gr} = [1-([CF]_r/33.3). (\%Q_r/\%Q_i]$, where $\%Q_i$ is the percentage of fluorescence quenching initially measured in vesicles before the addition of VA3 (see Appendix for details).

2.8. Light scattering

In addition to the CF release assays, light scattering was followed on an Aminco SPF 500C spectrofluorometer, with excitation and emission wavelengths both set at 530 nm and using a band-pass slit of 2.5 nm.

2.9. Determination of the VA3 critical micellar concentration (CMC)

The CMC was determined by use of the NPN fluorescence assay described by Rui et al. [29]. A 5 nM NPN solution in standard buffer, prepared from a stock solution of NPN in 99% EtOH, was stored at 21°C for 30 min before measuring the emission intensity. To determine the hypothetical CMC, different concentrations of VA3 (1, 5 and 15 μM) were added to the NPN solution and the emission inten-

Table 1
Characterization of the two distinct vesicle behaviors depending on the amount of VA3 added

Apparent $[VA3]_{introduced}$ (μM)	Corrected $VA3_{bound}$/POPS (R)	Initial slope of the CF release curve	Maximal CF release[a] (%)	Light scattering increase[b]
≤3.0	≤0.025	≠∞	<100	~0
≥7.5	≥0.070	∞	100	++

The total lipid amount was 30 μM.
[a]CF release was considered maximal when the release rate became equal to the control rate.
[b]Recorded after 24 h of incubation with VA3.

Table 2
Characterization of VA3-induced vesicle perturbations

Apparent $[VA3]_{introduced}$ (μM)	Apparent $VA3_{introduced}$/PS	CF release[a] (%)	Light scattering increase[a] (%)	Corrected $[VA3]_{introduced}$ (μM)	Corrected VA3/POPS (*R*)
1	0.1	40	−6	0.7	0.013
3	0.1	49	−5	2.3	0.025
6	0.1	51	5	5.1	0.035
10	0.1	53	14	9.0	0.045
7.5	0.25	79	40	6.5	0.070
15	0.5	100	75	13.9	0.081

The dashed line separates two different sets of experiments, depending on the apparent $VA3_{introduced}$/POPS ratio.
[a]Recorded after 24 h of VA3 incubation.

sities were compared to that measured in the absence of VA3. Fluorescence measurements were monitored on an Aminco SPF 500C spectrofluorometer. The excitation wavelength was set at 338 nm with a slitwidth of 4 nm and emission was monitored between 360 and 550 nm with a slitwidth of 5 nm.

3. Results

3.1. Monolayer experiments

3.1.1. Isochoric measurements

Isochoric measurements were carried out to determine the affinity of VA3, used at bulk concentrations ranging from 1 nM to 1 μM, for monomolecular films of POPC and POPS (Fig. 1). At a concentration of 0.15 μM, VA3 induced a 10 mN m^{-1} increase in the surface pressure of the POPS monolayers, i.e. a 100% increase of the initial surface pressure π^0 ($\pi^0 = 10$ mN m^{-1}). Saturation (200% increase) occurred at a concentration of 0.3 μM VA3. In contrast, only a slight film expansion was measured when VA3 was added to a POPC monolayer as the surface pressure increased by $< 80\%$ with 1 μM VA3. In the absence of phospholipids, VA3 also weakly affected the water surface tension due to its amphiphilic nature. However, the extent to which VA3 interacted with the air–water interface is not comparable with that measured on phospholipidic films, thus the affinity of VA3 for the interface essentially depends on its affinity for a lipidic surrounding, especially an acidic one.

Table 3
Mode of dye release

R	CF release[a] (%)	$\%Q_r^b$	$[CF]_r^c$ (mM)	$\%F_{gr}^d$
0.081	49	0.85	33.3	0
0.070	48	0.83	29.5	14
0.070	70	0.76	24.8	34
0.025	51	0.71	21.8	45
0.013	36	0.77	24.8	33
0	0	0.85	33.3	0

See Section 2 for details.
[a]Release recorded before passage of the vesicle suspension through a Sephadex column.
[b]$\%Q_r = 1 - I_0/I_{max}$.
[c]Obtained from a standard curve giving $\%Q$ as a function of initial encapsulated CF.
[d]$\%F_{gr} = [1 - ([CF]_r/33.3)\cdot(\%Q_r/0.85)]$.

3.1.2. Compression isotherm measurements

To evaluate further the role of electrostatic forces

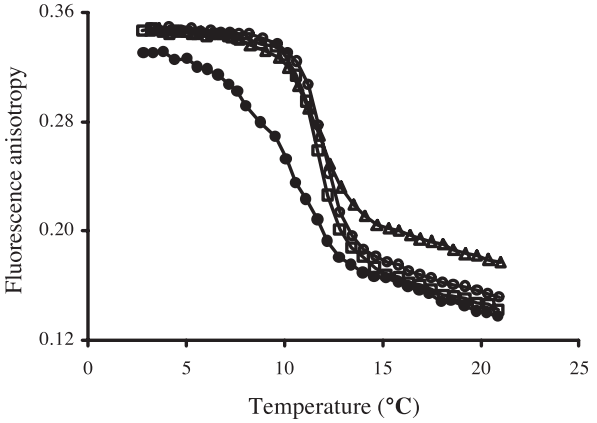

Fig. 5. Changes in the fluorescence anisotropy of a DPH probe incorporated into POPS $LUVET_{100}$ as a function of temperature. The anisotropy was measured without VA3 in the bulk (●), or with VA3 in *R* ratios of 0.025 (□) 0.070 (○) and 0.081 (△). Assays were carried out in duplicate.

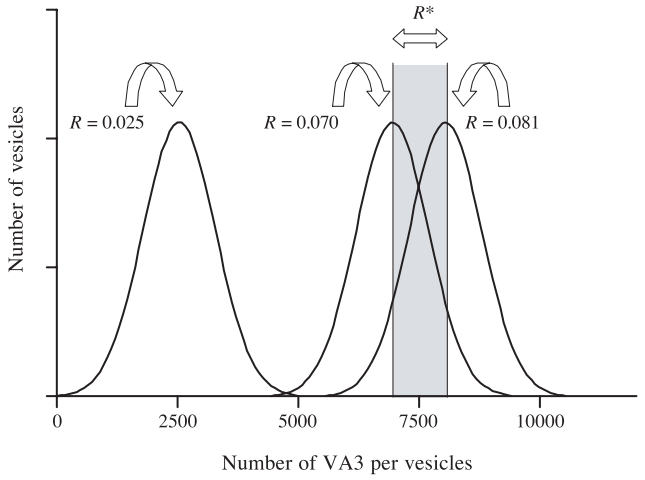

Fig. 6. Representation of the possible distributions of VA3 on vesicles. The distributions are Gaussian. The mean of each distribution is indicated by equivalent R values. Possible values of the discrete threshold ratio R^* fall in the area delimited by the dark rectangle. See text for details.

in the interaction of VA3 with phospholipidic monolayers, we monitored the compression isotherms of POPC and POPS monolayers in the presence of 0.1 μM VA3 at various ionic strengths (Fig. 2). VA3 notably increased the surface pressure of weakly organized POPC monolayers (apparent phospholipidic molecular area >100 Å^2) (Fig. 2A). By progressively restricting the monolayer area, this effect disappeared, showing that VA3 was being continuously expelled from the phospholipidic film. A *final exclusion surface pressure* close to 20 mN m^{-1} could be determined, which corresponds to the minimal pressure of a film that prevents the insertion of viscotoxin molecules. Increasing the ionic strength did not change the final exclusion surface pressure but it did increase the distribution of VA3 between the bulk solvent and the interface at larger apparent phospholipidic molecular areas. Surprisingly, VA3 was incorporated into weakly organized POPS monolayers to a similar extent (Fig. 2B). Moreover, increasing the ionic strength increased this phenomenon regardless of the phospholipid used: for both POPC and POPS films when the apparent phospholipidic molecular area was 120 Å^2, the surface pressure rose from 2 mN m^{-1} in the presence of 1 mM NaCl to 5 mN m^{-1} in the presence of 150 mM NaCl. Nevertheless, the expulsion pattern of VA3 from POPS films was quite different, depending on the bulk NaCl concentration. In the presence of 1 mM NaCl, VA3 was not excluded whereas with 150 mM NaCl VA3 was progressively excluded when the surface pressure exceeded 24 mN m^{-1}. In contrast with POPC films, the increase in ionic strength decreased the final exclusion surface pressure of the toxin from POPS monolayers.

In addition, some information can be drawn from the values determined for the final exclusion surface pressure, regarding the possible insertion of VA3 into phospholipidic bilayers. As the surface pressures evaluated for vesicles are usually between 25 mN m^{-1} [30] and 32 mN m^{-1} [31], VA3 cannot insert into POPC vesicles because the final exclusion surface pressure was only 20 mN m^{-1}. Despite the decrease in the final exclusion surface pressure that accompanied the increasing ionic strength, the higher values ($\geq$35 mN m^{-1}) recorded in POPS monolayers are consistent with at least the partial insertion of VA3 into POPS vesicles.

3.2. *$LUVET_{100}$ permeabilization: effect of the negative charge density*

The VA3-induced permeabilization of a set of POPC $LUVET_{100}$ containing increasing amounts of POPS was monitored by carrying out CF release assays to determine the effects of different negative charge densities on the permeabilization process. While no CF release could be recorded using pure POPC $LUVET_{100}$, the CF release readily increased as the amount of acidic phospholipids composing the $LUVET_{100}$ increased (data not shown).

3.3. *Interaction with POPS $LUVET_{100}$*

3.3.1. *Binding assays*

As the VA3-induced permeabilization of vesicles depends on the interaction of VA3 with POPS, binding assays were performed on pure POPS $LUVET_{100}$. To determine accurately the amount of VA3 bound to POPS vesicles, the strong adsorption of VA3 on the tube walls was taken into account. Up to 30% of the viscotoxin was adsorbed on the walls when a 1 μM solution of VA3 was used (Fig. 3). A similar behavior has been reported previously for other plant thionins [20,32]. We paid particular attention to this adsorption to determine the amount of VA3 actually available for the binding process, i.e. by sub-

tracting the amounts adsorbed to the wall from the added VA3. The resulting corrected POPS $LUVET_{100}$-VA3 binding curve (Fig. 3), expressed as the $VA3_{bound}$/POPS ratio (R), showed that values increased and reached saturation point when R was close to 0.075. These results also reflect a thermodynamic equilibrium as similar values were obtained after 10 min, 20 min, 12 h or 24 h in the same conditions.

3.3.2. Effects on bilayer integrity

3.3.2.1. CF release and light scattering studies. The addition of VA3 to POPS $LUVET_{100}$ caused a dose-dependent release of CF (Fig. 4), and induced slow, time-dependent, structural changes on the $LUVET_{100}$ as shown by light scattering measurements. Data dealing with the initial slope of the CF release curves, the maximum CF release, and the light scattering changes observed upon release (Table 1) revealed that the vesicles behave in two distinct ways depending on the amount of viscotoxin added.

3.3.2.2. The CF release is directly related to the amount of VA3 bound on the liposomes. The dose-dependent release of CF can be interpreted as a surface-dependent mechanism or a bulk concentration-dependent mechanism. A bulk concentration-dependent mechanism means that a critical bulk concentration of VA3 should result in an equilibrium between two structural states of VA3 in solution. The high structural stability displayed by thionins and viscotoxins in solution [33] means this should result in an equilibrium between monomeric and oligomeric states of VA3, the oligomers being more reactive towards the POPS vesicles. A similar behavior has already been reported for melittin analogues [34]. However, several lines of evidence argue against this bulk concentration threshold hypothesis: (i) the fluorescence characteristics (e.g. an increase in the fluorescent quantum yield or a blue shift of the maximum fluorescence wavelength) of NPN did not change significantly in the presence of up to 15 μM VA3, thus no micellar structures could be formed in these experimental conditions; (ii) nuclear magnetic resonance (NMR) studies on VA3 in solution did not detect any dimeric or oligomeric associations with up to 2 mM VA3 [4]. To prove that VA3 is unable to form unorganized aggregates, experiments were performed at a fixed apparent VA3/POPS ratio but with increasing apparent VA3 bulk concentrations. If the wall adsorption of VA3 is taken into account, both the CF release and the light scattering changes correlate well with the corrected $VA3_{bound}$/POPS ratio (R), whereas no correlation exists with the corrected bulk VA3 concentration (Table 2). Accordingly, CF release appears to be R-dependent, i.e. to depend on the VA3 concentration on the vesicle surface.

3.3.2.3. Mode of dye release. To elucidate the R-dependent CF release from the POPS vesicles, we investigated the extent of dye released by $LUVET_{100}$ exhibiting different VA3 surface concentrations. As previously reported by Weinstein et al. [28], dye may be released from vesicles by either an all-or-none or a gradual mode. In the former case, the dye is released as a result of the complete leakage of some vesicles, whereas in the latter case, the dye gradually leaks from all of the vesicles. The two modes can be distinguished by measuring the percentage of quenching remaining in the vesicles ($\%Q_r$) after they have lost a significant fraction of the dye. If the release depends on an all-or-none mode, $\%Q_r$ remains constant, otherwise, if it depends on an gradual mode, $\%Q_r$ decreases by an amount that can be measured by a standard quench curve. This standard curve was also used to calculate the predictable equivalent gradual release (see Appendix for details). As shown in Table 3, the CF release was mainly a gradual one when $R \leq 0.025$, but it followed a strictly all-or-none mode when R reached 0.081, at least in the experimental conditions resulting in 50% CF release. This all-or-none mode also accounted for the 50% release that occurred when R was 0.070. Thus, the mode of CF release differs according to the R ratio. The transition from one mode of release to the other occurred for an R value between 0.025 and 0.070.

However, when R was 0.070, the mode of release was more complex; it was mainly an all-or-none process at the beginning of the interaction and became more gradual afterwards. In fact, for this R value, the CF release increased by 22%, which is very similar to the 20% increase predicted. This means that the process involves a time-dependent change from an all-or-none response to a gradual release.

3.3.3. POPS $LUVET_{100}$ fluorescence polarization

The fluorescence polarization of DPH incorporated in POPS $LUVET_{100}$ was measured to investigate the effect of VA3 on the overall phospholipid organization. POPS bilayers usually showed a broad gel-to-fluid transition at around 8–12°C but, in the presence of VA3, three distinct changes occurred (Fig. 5): (i) the probe in the phospholipidic gel phase behaved in a more constrained manner, (ii) the cooperativity of the gel to fluid transition increased, and (iii) the constraints on the probe in a phospholipidic fluid state increased, although this was highly dependent on the *R* ratio value. These changes reveal that the VA3–lipid complex became more organized. A similar behavior was observed when β-DPH-HPC was used as a probe (data not shown), suggesting that the constraining effect of VA3 readily affects the hydrophobic core of the phospholipid bilayer.

4. Discussion

4.1. Phenomena involved in the approach and the insertion of VA3 in POPC and POPS monolayers

As previously reported for other thionins, our results show that VA3 has a high affinity for phospholipidic surroundings. This is consistent with the overall structural features of this plant toxin, which is highly amphipathic [4]. As proposed for other thionins [20,22,35], the electropositive character of VA3 (+6) may play an essential role in the interaction with both model and plasma membranes. However, the electrostatic component of thionins has been suggested to only participate in the first step of their interaction with membranes [5,22]. In this respect, two major results can be drawn from the analysis of the compression isotherms shown in Fig. 2: (i) changes in the surface pressure were induced by VA3 in the large apparent phospholipidic areas. These reflect the affinity of the toxin towards weakly organized lipid films. Similarly surface pressure was increased at higher ionic strengths regardless of the phospholipid (acidic or zwitterionic) used. Thus, the electrostatic component of VA3 does not appear to participate in the bulk–membrane partition process; (ii) in contrast, the analysis of the final exclusion surface pressure of VA3, which is related to the stability of the toxin in the lipid film, showed that VA3 is only efficiently inserted into acidic phospholipid monolayers and that this insertion is destabilized by an increase in the ionic strength. This strongly suggests that the electrostatic component is involved in the insertion of VA3 into lipid films.

Accordingly, we favor a salting out process, due to the amphipathic nature of the toxin, that allows the toxin to adsorb to the lipid membrane regardless of its phospholipid (acidic or zwitterionic) composition. Further insertion and membrane perturbation can only take place if the appropriate electrostatic interactions occur. Accordingly, POPC $LUVET_{100}$ must contain more than 10% POPS to release significant amounts of CF after 10 min in the presence of VA3 (data not shown). Both results are consistent with previous observations showing that even though thionins bind to egg PC vesicles, no subsequent permeabilization could be detected [20].

4.2. The interaction of VA3 with POPS vesicles is governed by a threshold ratio mechanism

Data obtained from model POPS membranes, i.e. in which the CF release, light scattering and fluorescence polarization changes are induced by VA3, indicate that the vesicles change in a *R*-dependent way, in the range between $R \in]0.025{:}0.07[$. When $R \leq 0.025$, only partial CF release occurred and neither structural changes of vesicles nor an increase in the DPH anisotropy in the POPS fluid phase could be detected. Conversely, at higher *R* values, the CF release was complete and associated with both structural modifications of the vesicles and an increased DPH anisotropy in the POPS fluid phase. Such dose-dependent changes of DPPG vesicles in the presence of an α-thionin have been already reported to occur when the apparent protein–lipid ratio is 0.008 [20]. *Pyrularia* thionin also induced the aggregation of DPPG vesicles at an apparent threshold value of 0.1 for the protein–lipid ratio [22], and Thevissen et al. [8] reported that >0.2 μM of α-hordothionin are needed to induce signals that can be recorded by the black lipid membrane apparatus. However, with the large range of *R* values used here, the behavior is not so clear-cut. This is shown in Table 2, where light scattering reveals some perturbations when *R* exceeds

0.035. Likewise, Table 3 shows that, with the exception of $R = 0.081$, it is not possible to describe fully the CF release, which appears to be mainly but not exclusively governed by a gradual or an all-or-none mode of dye release. Nevertheless, we will show that these observations are more consistent with a threshold ratio hypothesis than with a continuous dose dependence hypothesis.

The change observed in the mode of CF release when $R = 0.070$ (Table 3) does not depend on a gradual change in the amount of VA3 bound to vesicles as this binding was shown to be complete after 10 min of incubation. This implies that in these experimental conditions some vesicles released all of their dye, i.e. bursting of the lipid bilayer, whereas other vesicles only displayed a slower enhanced permeability. The occurrence of some heterogeneity in the size or composition of our POPS vesicles could account for a more specific recognition of a few vesicles by VA3. Accordingly, we carefully ensured that both the working POPS solution and the freshly prepared POPS vesicles were free of lysophospholipids. The size of POPS liposomes was also checked by QELS to confirm that they were homogeneously distributed (see Section 2). This means it is unlikely that heterogeneity could occur in the POPS vesicle preparations.

If it is assumed that there is both a uniform size distribution of vesicles and a random distribution of VA3 on the vesicle surface, this latter distribution can be described as having a Gaussian distribution because of the large number of vesicles and the large average number of bound VA3 [36]. This distribution is based on the average number of VA3 bound per vesicle, which is, in turn, related to the R ratio (Fig. 6). As some vesicles are lysed and others remain intact (but display an enhanced permeabilization), it can be assumed that a minimal number of VA3 molecules must be bound to one vesicle to trigger all-or-none leakage [36,37]. This number can be divided by the number of POPS molecules in a 100 nm diameter vesicle (if 55 $Å^2$ is the molecular area of POPS, 1×10^5 POPS molecules are estimated to constitute the 4 nm thick bilayer of a 100 nm vesicle), as a simple way of estimating a *discrete threshold ratio* R^*. Given that the measured all-or-none mode dye release accounted for less than 50% of the total dye release when R was 0.070 and more than 50% when R was 0.081 (Table 3), the R^* value should be between 0.070 and 0.081, which corresponds to 7000 (0.070) and 8000 (0.081) VA3 molecules per $LUVET_{100}$.

As VA3 molecules are thought to interact with phospholipid bilayers via two amphipathic adjacent α-helices [38] with a molecular surface of about 400 $Å^2$, one VA3 molecule can cover an area corresponding to seven POPS molecules. As the bilayer is 4 nm thick, 54% of POPS are estimated to form the outer leaflet of the POPS vesicle bilayer, so that about 7700 VA3 molecules should totally cover one POPS vesicle. The calculated R^* value (0.077) is in the range of previously estimated R^* values (0.070–0.081). Accordingly, the total permeabilization of one POPS vesicle would be directly related to its complete coverage by VA3 molecules in a monolayer. This is similar to what has already been reported for other membrane-active peptides dermaseptin [39] and cecropin [40]. A threshold R^* ratio has been proposed for other peptides, such as magainin and protegrin [41]. Furthermore, assuming a fixed discrete threshold R^* value, the all-or-none contribution to CF release can logically occur for a wide range of R values, depending on the width of the VA3 distribution on the POPS vesicles.

4.3. Localization of VA3 in the POPS bilayer

So, VA3 presumably interacts with POPS vesicles in a 'carpet-like' fashion [42]. Nevertheless, it paradoxically stiffens and modifies the polymorphism properties of the POPS bilayer, which is not usually described for peptides with 'carpet-like' interactions [42,43]. On the contrary, other membrane-active peptides usually enhance the disorder of the gel phase bilayer, as reported for melittin [44], cardiotoxin [45] and, to a lesser extent, for magainin [46]. Moreover, as shown for cardiotoxin, an increase in gel phase disorder and a decrease in the gel to liquid phase transition cooperativity are related with the insertion of the toxin in the vicinity of the phosphate groups of the phospholipids and are associated with the entry of water molecules into the bilayer. Likewise, the observation of the stiffening effect of VA3 on POPS bilayer gives us an indication on the extent of the VA3 insertion. The polymorphism properties of POPS bilayers essentially result from intermolecular H-bonds due to the three electronegative groups of

the polar head together with the hydration by water molecules [47,48]. Moreover, unlike the ammonium, phosphate and ester groups that participate in intermolecular H-bonds and are thus partly responsible for the phospholipid cohesion [47–50], serine carboxylic groups mainly develop electrostatic repulsions. MD calculations on the effect of Li^+ on a PS bilayer showed that the charge screening effect and dehydration in the vicinity of serine carboxylic groups are related to an increase of the PS bilayer order [51]. In addition, the removal of water molecules from the acidic lipid bilayers associated with the stabilization of the gel phase apparently concerns the hydration by water from the carboxyl groups of the serine heads [47]. Furthermore, thionins were shown to reduce the amount of water associated with polar heads of the S49 cell plasma membrane phospholipids and the movement of this water [9]. Consequently, if we assume that the electrostatic component mainly accounts for the anchoring of VA3 with POPS, the resulting stiffening of the phospholipid bilayer presumably arises from either the direct interaction with the carboxylic groups of the serine heads and/or the movement of water molecules out of the bilayer.

4.4. Permeabilization of POPS vesicles is due to bilayer defects

^{31}P-NMR measurements performed on PC:PS (8:2) vesicles in the presence of *Pyrularia* thionin led Gasanov et al. [21] to propose that the thionins directly interact with some PS molecules which may lead to non-bilayer-organized local domains and bilayer degradation. Likewise, if we consider that VA3 binds POPS vesicles electrostatically and triggers the stiffening of the lipid bilayer, the toxin may be able to create clusters of motionally restricted lipids in the bilayer. The occurrence of such peptide-induced clusters is far from unusual in PS phospholipids interacting with basic peptides or proteins [52,53]. The peptide-induced clusters would mimic phospholipids at temperatures near to the gel to fluid transition temperature, which is characterized by coexisting gel and fluid lipid domains [54]. It is noteworthy that this transition temperature is associated with an increase in permeability [55], as a result of bilayer defects occurring at the interface of the gel and the fluid lipid domains [54]. This is consistent with the gradual release of the dye from POPS vesicles induced by VA3 below the R^* threshold value, which would depend on bilayer defects occurring at interfacial regions of the clusters, rather than on VA3-induced pores. This mechanism is in agreement with the in-plane diffusion model reported by Bechinger [56]. Furthermore, the complete covering of POPS vesicles by VA3 molecules would result in two opposite effects: a stiffening of the lipid bilayer due to the VA3 layer and Brownian agitation, which tends to fluidify the bilayer. Similarly, given that both VA3 and POPS are electrically charged, some lateral repulsion should occur between peptides at high R ratio values, whereas basic viscotoxins should compete in recruiting charged lipids in their immediate vicinity [53]. As a result, the vesicles should display some instability, which could result in the rupture of bilayers and further vesicle rearrangements that are partly responsible for the increase in light scattering at high R ratio values.

4.5. Viscotoxin A3 and eukaryotic cells

To conclude, we will discuss the biological reliability of our results obtained on model POPS bilayers, which require PS molecules to occur on the outer leaflet of the plasma membrane so that VA3 can interact with tumor cells and disturb their permeability. Although PS, which accounts for 10–15% of total membrane phospholipids, is usually reported to be concentrated in the inner leaflet of the lipid bilayer of erythrocytes [57], some compelling evidence exists for a different distribution in other cell types. It has been shown that 10–20% of PS are present in the outer leaflet of erythroblasts [58,59] and that up to 10% are in BHK-21 cells [60]. Interestingly, undifferentiated tumorigenic murine and human cells express 7–8-fold more PS in the outer leaflet than their non-tumorigenic counterparts [61,62]. These discrepancies may account for the distinct activity of VA3 towards erythrocytes and tumor cells. In addition, given that a eukaryotic plasma membrane contains about 1×10^8 phospholipid molecules and 10% PS, a simple calculation shows that if only 0.5% of the PS occurs on the outer leaflet, the amount of exposed PS is similar to that on one $LUVET_{100}$. Moreover, according to Schaller et al. [23], cytotoxic activity was mea-

sured with 1×10^{-7} M VA3 for 1×10^{6} cells, which gives an apparent molecular ratio (1×10^{3} VA3/1 PS) 2000-fold higher than the highest ratio we used in this study. Thus, we hypothesize that peptide-induced lipid clusters could occur in the outer leaflet of the plasma membrane and that they are responsible for further membrane perturbations leading to cell death. This hypothesis is currently under investigation in the laboratory.

Acknowledgements

The financial support of the CNRS is gratefully acknowledged.

Appendix

For 30 μM $LUVET_{100}$ with CF encapsulated at a concentration of X mM:

$$I_{0,X} = n_X \cdot i_{Q,X} \tag{A1}$$

$$I_{\max,X} = n_X \cdot i_D \tag{A2}$$

where n_X represents the number of molecules of CF encapsulated in 30 μM $LUVET_{100}$ containing X mM CF, $I_{0,X}$ is the line-base fluorescence intensity of 30 μM $LUVET_{100}$ containing X mM CF, $I_{\max,X}$ is the fluorescence intensity of 30 μM $LUVET_{100}$ containing X mM CF after the addition of TX100, $i_{Q,X}$ is the average fluorescence intensity of one CF molecule in high concentration (X mM) conditions (this fluorescence is partially quenched and depends on the value of X) and i_D is the average fluorescence intensity of one CF molecule in infinitely diluted condition (in this study, this condition was obtained after the addition of TX100 and was independent of the value of X).

We always started with $LUVET_{100}$ containing 33.3 mM CF, thus the percentage released (%F) equals:

$$\%F = \frac{I_t - I_{0,33.3}}{I_{\max,33.3} - I_{0,33.3}} \tag{A3}$$

where I_t is the fluorescence intensity recorded at time t.

If the release is gradual leading to vesicles containing X mM CF ($X < 33.3$), we obtain:

$$I_t = I_{0,X} + (n_{33.3} - n_X) \cdot i_D = I_{0,X} + I_{\max,33.3} - I_{\max,X} \tag{A4}$$

Thus, in these conditions, we can calculate the equivalent gradual release (%F_{gr}):

$$\%F_{gr} = \frac{(I_{0,X}/I_{\max,X}) + (I_{\max,33.3}/I_{\max,X}) - 1 - (I_{0,33.3}/I_{\max,X})}{1-(I_{0,33.3}/I_{\max,33.3})} \cdot (I_{\max,X}/I_{\max,33.3}) \tag{A5}$$

If all $LUVETs_{100}$ have the same intravesicular volume:

$$I_{\max,X}/I_{\max,33.3} = \frac{n_X}{n_{33.3}} = \frac{X}{33.3} \tag{A6}$$

and

$$I_{0,33.3}/I_{\max,X} = \frac{I_{0,33.3}}{n_X \cdot i_D} = \frac{n_{33.3} \cdot I_{0,33.3}}{n_X \cdot I_{\max,33.3}} = \frac{33.3}{X} \cdot (I_{0,33.3}/I_{\max,33.3}) \tag{A7}$$

Moreover, according to the definition of the percentage of fluorescence quenching remaining in the vesicles before (%Q_i) or after the release has occurred (%Q_r):

$$\%Q_r = I - I_{0,X}/I_{\max,X} \tag{A8}$$

$$\%Q_i = 1 - I_{0,33.3}/I_{\max,33.3} \tag{A9}$$

Finally, by combining Eq. A5 with Eqs. A6–A9, we obtain:

$$\%F_{gr} = 1 - \frac{[CF]_r}{33.3} \cdot \frac{\%Q_r}{\%Q_i} \tag{A10}$$

where $[CF]_r$ is the residual concentration of CF in the vesicles after the release.

References

[1] W.A. Hendrickson, M.M. Teeter, Nature 290 (1981) 107–113.

[2] G.M. Clore, M. Nilges, D.K. Sukumaran, A.T. Brünger, M. Karplus, A.M. Gronenborn, EMBO J. 5 (1986) 2729–2735.
[3] M.M. Teeter, X.Q. Ma, U. Rao, M. Whitlow, Proteins 8 (1990) 118–132.
[4] S. Romagnoli, R. Ugolini, F. Fogolari, G. Schaller, K. Urech, M. Giannattasio, L. Ragona, H. Molinari, Biochem. J. 350 (2000) 569–577.
[5] D.E. Florack, W.J. Stiekema, Plant Mol. Biol. 26 (1994) 25–37.
[6] J.M. Caaveiro, A. Molina, J.M. Gonzalez-Manas, P. Rodriguez-Palenzuela, F. Garcia-Olmedo, F.M. Goni, FEBS Lett. 410 (1997) 338–342.
[7] P. Hughes, E. Dennis, M. Whitecross, D. Llewellyn, P. Gage, J. Biol. Chem. 275 (2000) 823–827.
[8] K. Thevissen, A. Ghazi, G.W. De Samblanx, C. Brownlee, R.W. Osborn, W.F. Broekaert, J. Biol. Chem. 271 (1996) 15018–15025.
[9] H.A. Wilson, W. Huang, J.B. Waldrip, A.M. Judd, L.P. Vernon, J.D. Bell, Biochim. Biophys. Acta 1349 (1997) 142–156.
[10] J. Konopa, J.M. Woynarowski, M. Lewandowska-Gumieniak, Hoppe Seylers Z. Physiol. Chem. 361 (1980) 1525–1533.
[11] M.L. Jung, S. Baudino, G. Ribereau-Gayon, J.P. Beck, Cancer Lett. 51 (1990) 103–108.
[12] K. Urech, G. Schaller, P. Ziska, M. Giannattasio, Phytother. Res. 9 (1995) 49–55.
[13] G.E. Evett, D.M. Donaldson, L.P. Vernon, A.M. Judd, R.M. MacLeod, W.S. Fracki, D. Li, N. Owen, C. Perry, G.H. Naisbitt, Toxicon 24 (1986) 622–625.
[14] A. Bussing, G.M. Stein, M. Wagner, B. Wagner, G. Schaller, U. Pfuller, M. Schietzel, Eur. J. Biochem. 262 (1999) 79–87.
[15] J. Evans, Y.D. Wang, K.P. Shaw, L.P. Vernon, Proc. Natl. Acad. Sci. USA 86 (1989) 5849–5853.
[16] V.R. Osorio e Castro, B.A. van Kuiken, L.P. Vernon, Toxicon 27 (1989) 501–510.
[17] P.G. Lankisch, W. Vogt, Experientia 27 (1971) 122–123.
[18] V.R. Osorio e Castro, L.P. Vernon, B.A. Van Kuiken, Toxicon 27 (1989) 511–517.
[19] F. Wang, G.H. Naisbitt, L.P. Vernon, M. Glaser, Biochemistry 32 (1993) 12283–12289.
[20] J.M. Caaveiro, A. Molina, P. Rodriguez-Palenzuela, F.M. Goni, J.M. Gonzalez-Manas, Protein Sci. 7 (1998) 2567–2577.
[21] S.E. Gasanov, L.P. Vernon, T.F. Aripov, Arch. Biochem. Biophys. 301 (1993) 367–374.
[22] W. Huang, L.P. Vernon, L.D. Hansen, J.D. Bell, Biochemistry 36 (1997) 2860–2866.
[23] G. Schaller, K. Urech, M. Giannattasio, Phytother. Res. 10 (1996) 473–477.
[24] C.W. McClare, Anal. Biochem. 39 (1971) 527–530.
[25] K. Nicolay, A.M. Sautereau, J.F. Tocanne, R. Brasseur, P. Huart, J.M. Ruysschaert, B. de Kruijff, Biochim. Biophys. Acta 940 (1988) 197–208.
[26] M.J. Hope, M.B. Bally, G. Webb, P.R. Cullis, Biochim. Biophys. Acta 812 (1985) 55–65.
[27] N. Leborgne, L. Dupou-Cezanne, C. Teulières, H. Canut, J.F. Tocanne, A.M. Boudet, Plant Physiol. 100 (1992) 246–254.
[28] J.N. Weinstein, E. Ralston, L.D. Leserman, R.D. Klausner, P. Dragsten, P. Henkart, R. Blumenthal, in: G. Gregoriadis (Ed.), Liposome Technology, Vol. 3, CRC Press, Boca Raton, FL, 1984, pp. 183–203.
[29] M. Rui, M. Brito, L. Winchil, C. Vaz, Anal. Biochem. 152 (1986) 250–255.
[30] H. Schindler, Biochim. Biophys. Acta 555 (1979) 316–336.
[31] A. Seelig, Biochim. Biophys. Acta 899 (1987) 196–204.
[32] L.P. Vernon, A. Rogers, Toxicon 30 (1992) 701–709.
[33] J.H. Park, C.K. Hyun, H.K. Shin, Cancer Lett. 139 (1999) 207–213.
[34] E. John, F. Jahnig, Biophys. J. 63 (1992) 1536–1543.
[35] K. Wada, Y. Ozaki, H. Matsubara, H. Yoshizumi, J. Biochem. 91 (1982) 257–263.
[36] T. Benachir, M. Lafleur, Biochim. Biophys. Acta 1235 (1995) 452–460.
[37] R.A. Parente, S. Nir, F.C. Szoka Jr., Biochemistry 29 (1990) 8720–8728.
[38] I. Kelly, M. Pézolet, D. Marion, Biophys. J. 74 (1998) A309.
[39] Y. Pouny, D. Rapaport, A. Mor, P. Nicolas, Y. Shai, Biochemistry 31 (1992) 12416–12423.
[40] E. Gazit, A. Boman, H.G. Boman, Y. Shai, Biochemistry 34 (1995) 11479–11488.
[41] H.W. Huang, Biochemistry 39 (2000) 8347–8352.
[42] Y. Shai, Biochim. Biophys. Acta 1462 (1999) 55–70.
[43] E. Gazit, I.R. Miller, P.C. Biggin, M.S. Sansom, Y. Shai, J. Mol. Biol. 258 (1996) 860–870.
[44] J.F. Faucon, E. Bernard, J. Dufourcq, M. Pezolet, P. Bougis, Biochimie 63 (1981) 857–861.
[45] A. Desormeaux, G. Laroche, P.E. Bougis, M. Pezolet, Biochemistry 31 (1992) 12173–12182.
[46] K. Matsuzaki, M. Harada, S. Funakoshi, N. Fujii, K. Miyajima, Biochim. Biophys. Acta 1063 (1991) 162–170.
[47] G. Cevc, A. Watts, D. Marsh, Biochemistry 20 (1981) 4955–4965.
[48] J.M. Boggs, Biochim. Biophys. Acta 906 (1987) 353–404.
[49] J.J. Lopez Cascales, H.J.C. Berendsen, J. Garcia de la Torre, J. Phys. Chem. 100 (1996) 8621–8627.
[50] J.J. Lopez Cascales, J. Garcia de la Torre, S.J. Marrink, H.J.C. Berendsen, J. Chem. Phys. 104 (1996) 2713–2720.
[51] J.J. Lopez Cascales, J. Garcia de la Torre, Biochim. Biophys. Acta 1330 (1997) 145–156.
[52] A. Hinderliter, P.F. Almeida, C.E. Creutz, R.L. Biltonen, Biochemistry 40 (2001) 4181–4191.
[53] S. May, D. Harries, A. Ben-Shaul, Biophys. J. 79 (2000) 1747–1760.
[54] L. Cruzeiro-Hansson, O.G. Mouritsen, Biochim. Biophys. Acta 944 (1988) 63–72.
[55] D. Papahadjopoulos, K. Jacobson, S. Nir, T. Isac, Biochim. Biophys. Acta 311 (1973) 330–348.
[56] B. Bechinger, Biochim. Biophys. Acta 1462 (1999) 157–183.

[57] A.J. Verkleij, R.F. Zwaal, B. Roelofsen, P. Comfurius, D. Kastelijn, L.L. van Deenen, Biochim. Biophys. Acta 323 (1973) 178–193.
[58] P.H. van der Schaft, B. Roelofsen, J.A. Op den Kamp, L.L. van Deenen, Biochim. Biophys. Acta 900 (1987) 103–115.
[59] A. Rawyler, P.H. van der Schaft, B. Roelofsen, J.A. Op den Kamp, Biochemistry 24 (1985) 1777–1783.
[60] F. Leterrier, C. Gary-Bobo, in: Hermann (Ed.), Biologie Membranaire, Structure et Dynamique des Membranes Biologiques, Herman Ed., Paris, 1989, p. 51.
[61] J. Connor, C. Bucana, I.J. Fidler, A.J. Schroit, Proc. Natl. Acad. Sci. USA 86 (1989) 3184–3188.
[62] T. Utsugi, A.J. Schroit, J. Connor, C.D. Bucana, I.J. Fidler, Cancer Res. 51 (1991) 3062–3066.